Joint Pathology Center
Veterinary Pathology Services

**WEDNESDAY SLIDE
CONFERENCE 2019-2020**

C o n f e r e n c e 18

12 Feb 2020

Timothy Cooper, DVM, PhD DACVP
Pathology Department
NIH/NIAID
Integrated Research Facility
Frederick, MD

CASE I: 17-325 (JPC 4105224).

**Signalment:** 8-month, male intact Old English Sheepdog, *Canis familiaris*, dog

History: The dog was presented to the Internal Medicine Service for evaluation of a 4 month period of daily vomiting, frequent diarrhea, depression following meals, and lack of weight gain.

Gross Pathology: A large mass of vessels was seen surrounding gallbladder and infiltrating into the liver at surgery. A biopsy including the gallbladder, vessels, and adjacent hepatic parenchyma was submitted for histopathology.

Laboratory results: Serum chemistry revealed elevations in activity of ALP (204 IU/L) and ALT (76 IU/L); serum ammonia concentration was elevated at 40 umol/L. Complete blood count revealed a moderate, normocytic, normochromic anemia with a

hematocrit of 24.6%. A CT confirmed the presence of a large arterioportal malformation centered at the gallbladder and falciform fat as well as multiple acquired extrahepatic portosystemic shunts, moderate ascites, and left-sided liver atrophy.

Microscopic Description: Liver, gall bladder: Two sections of liver and gallbladder are examined. Surrounding the common bile duct and gall bladder is a mass-like proliferation of numerous
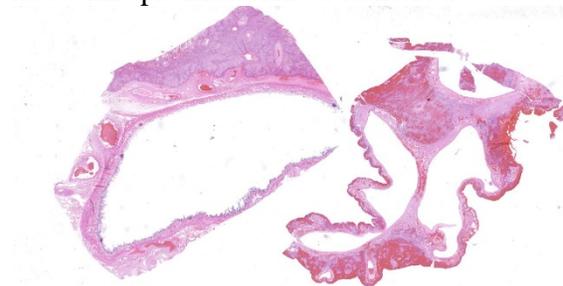
Liver, dog. Two sections of liver are presented. The section at left has a markedly dilated gallbladder within; the section at right contains multiple sections of a markedly dilated and tortuous muscular artery with a 10mm diameter. (HE, 5X)
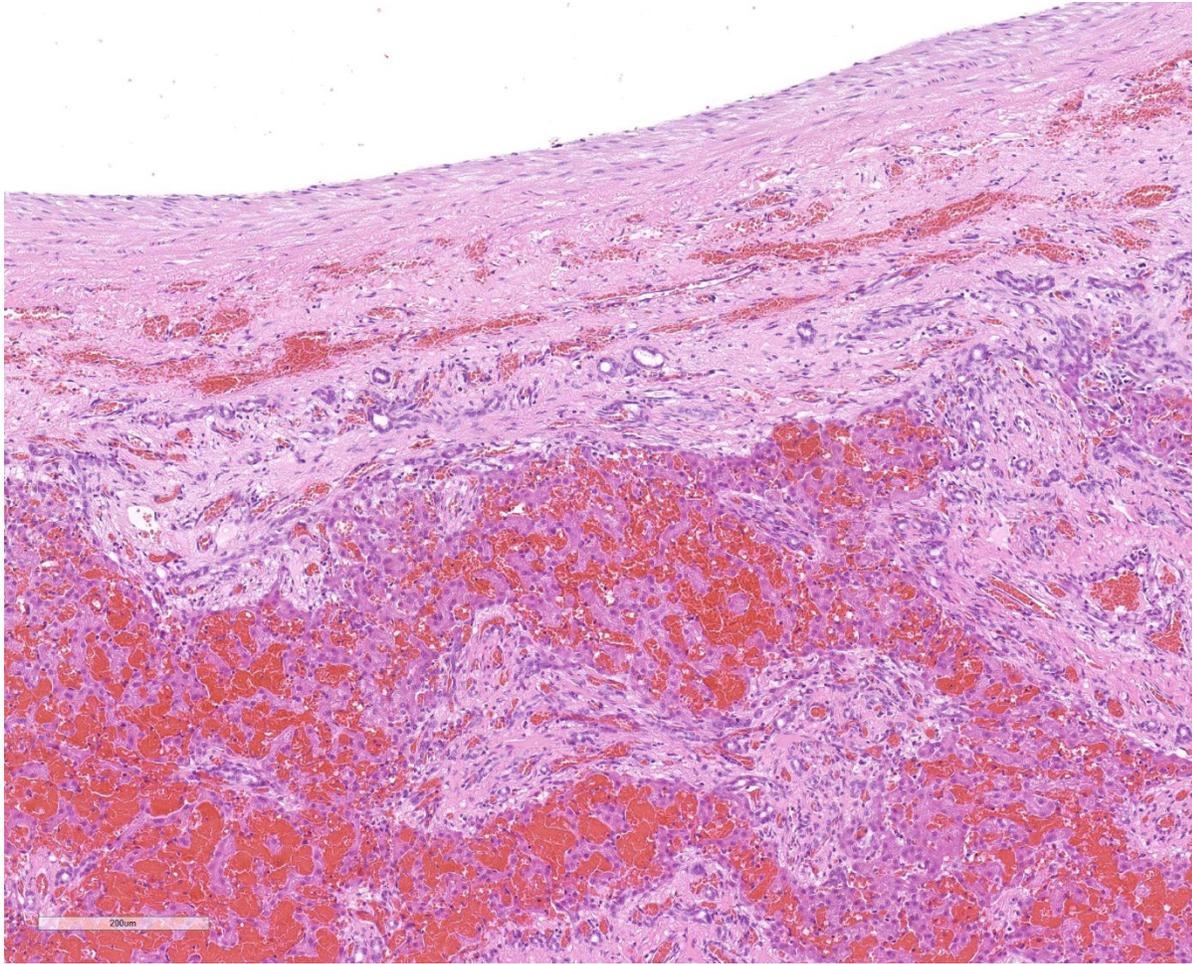
Liver, dog. Higher magnification of the wall of the arteriovenous connection. From top – smooth muscle cells of the wall are separated by abundant fibrillar collagen, with extends into the adjacent adventitia, effacing the tunica externa. This fibrosis extends into the adjacent parenchyma, replacing hepatocytes and entrapping bile ductules. Peripherally, there is marked fibrosis and arteriolar and ductular hyperplasia within portal areas which extends into the adjacent parenchyma, and severe dilation of hepatic sinusoids. (HE, 127X)

tortuous, small to large, well-differentiated arteries and veins, which rarely anastomose, and dissect or compress the hepatic parenchyma. The endothelium of veins and arteries is occasionally hypertrophied. Arterial and arteriolar walls are diffusely moderately thickened by subintimal edema, pale basophilic, mucinous matrix, and irregular fibers as well as by moderate to marked smooth muscle hypertrophy of the tunica media. The internal elastic lamina is frequently fragmented or absent (confirmed by Verhoeff-Van Gieson stain). The walls of veins and venules are markedly thickened and resemble arteries (arterialization). There is expansion of the tunica intima by irregular fibers and the tunica media by smooth muscle hypertrophy. The lymphatics surrounding the abnormal arteries and veins, those deep to the hepatic capsule, within portal tracts, and surrounding central veins are frequently moderately to markedly ectatic. The adjacent hepatic parenchyma is compressed by the vessels, with multifocal atrophy of the hepatic lobules. Additionally, there are

markedly increased numbers of bile duct profiles in portal tracts and isolated within the hepatic parenchyma; these bile ducts are frequently surrounded by concentric lamellar fibrosis ("onion-skinning") . Portal tracts also have increased numbers of small arteriolar profiles and portal vein profiles are largely absent. Centrilobular hepatocytes are frequently atrophied and diffusely, hepatocytes are mildly to moderately swollen by diaphanous vacuolar change (glycogen type). Scattered throughout the parenchyma are individual necrotic hepatocytes. There is moderate stellate cell hypertrophy; hypertrophied stellate cells frequently contain large, clear, spherical vacuoles (lipid).

Contributor's Morphologic Diagnosis:

Liver, gallbladder: Arteriovenous fistula with multifocal hepatic compression and atrophy, marked biliary and arteriolar hyperplasia, portal vein hypoperfusion, and moderate, diffuse glycogen-type hepatic vacuolation

Contributor's Comment: The diagnostic imaging, gross and histologic findings of this biopsy sample are consistent with a diagnosis of a hepatic arteriovenous fistula. Arteriovenous (AV) fistulae can be
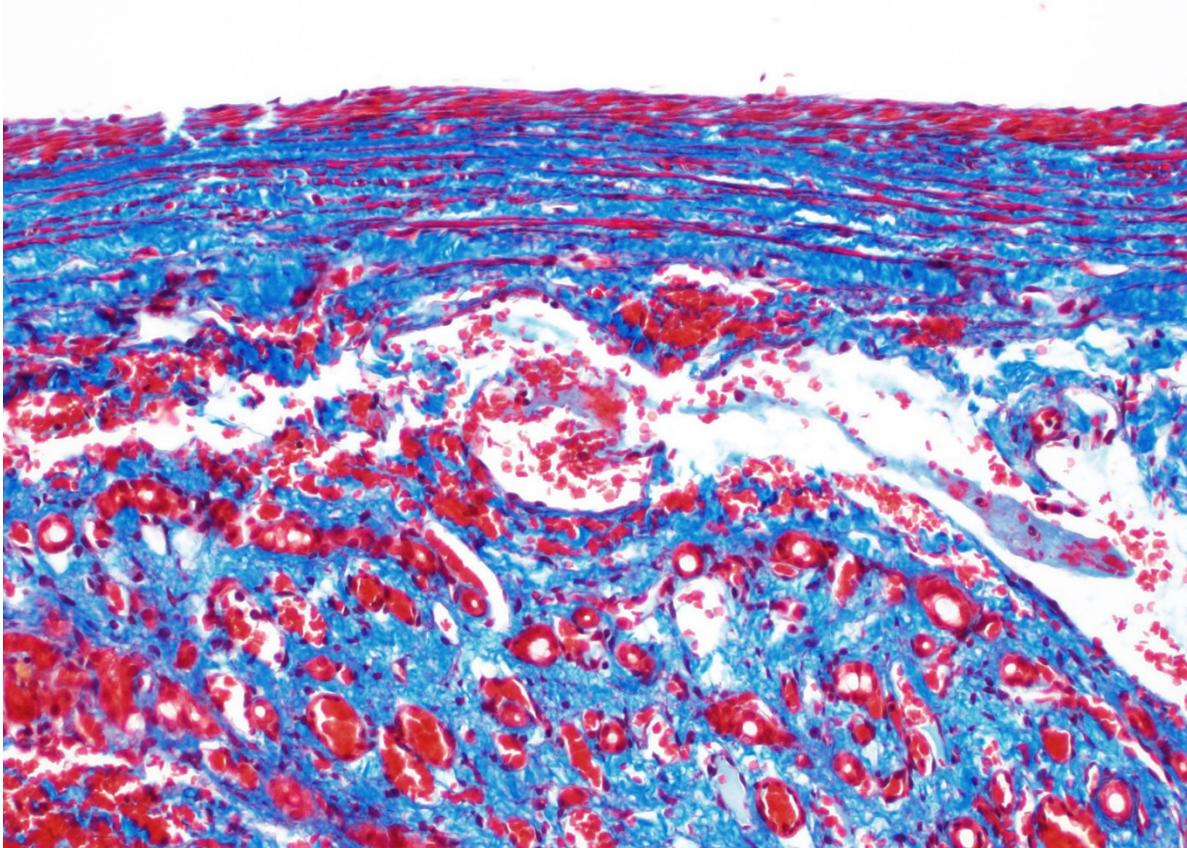
Liver, dog. A Masson's trichrome stain demonstrates the large amount of collagen within the wall of the fistula. (HE, 400X)
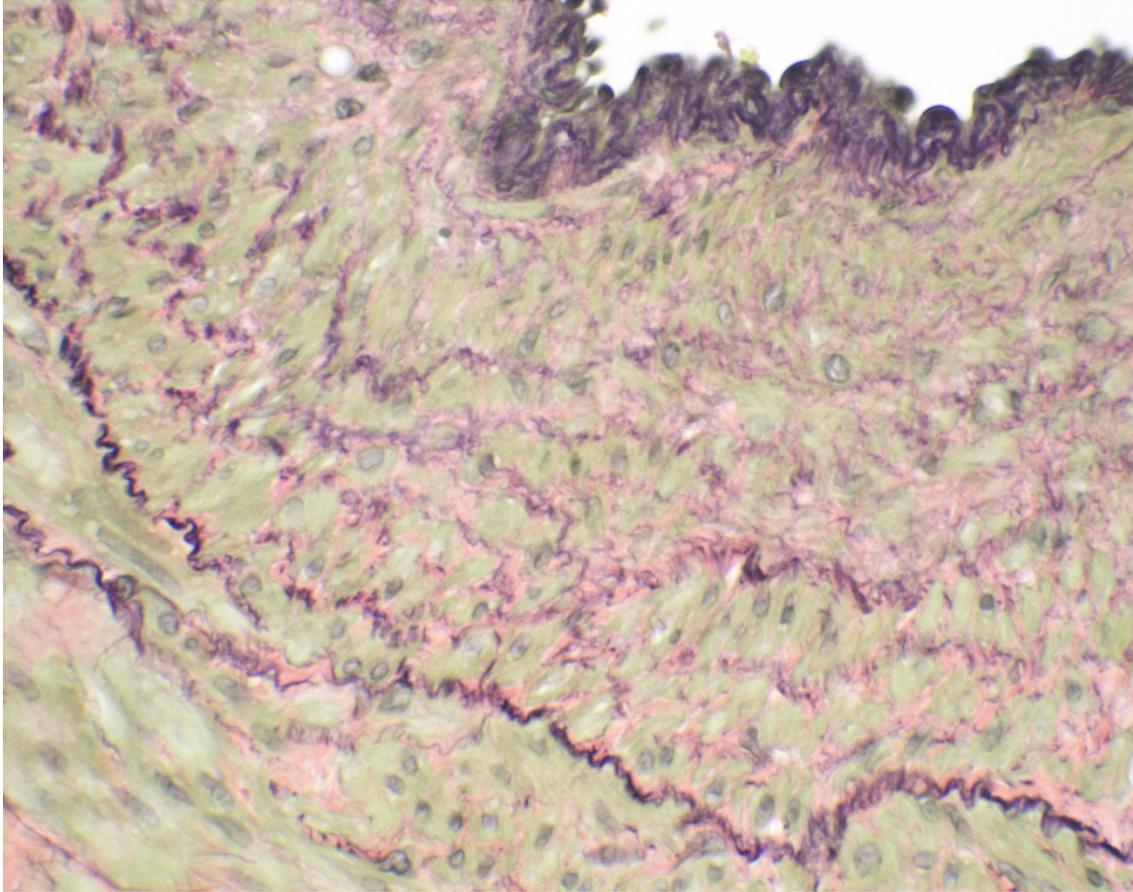
Liver, dog. A Verhoeff-van Gieson stain demonstrates the lack of an internal elastic lamina as well as deposition of elastin fibers between smooth muscle cells in the media (Verhoef- van Gieson, 400X)

congenital or acquired; acquired AV fistulae are documented to occur following trauma, rupture of arterial aneurysms into a vein, inflammation or necrosis of adjacent vessels, and iatrogenically (typically surgical intervention) [3,5,6]. AV fistulae have been reported in a variety of locations, including intrahepatic, pulmonary, and on the limbs.[3,6] They have been reported in dogs, cats, horses, cattle, and humans.[3,6]

Clinical signs of AV fistulae depend on the location; typically signs are associated with increased hydrostatic pressure within veins and subsequent increased intra-lymphatic pressure.[3,6] In fistulae involving abnormal

blood flow to the liver, ascites, hepatic encephalopathy and synthetic liver failure can occur, resulting in depression, seizures, vomiting, and diarrhea. [2,3,6,9,12]

Gross findings of AV fistulae usually show one or more anastomoses of a large vein and large artery, surrounded by a tangle of medium and small arteries and venules that contribute to a mass effect. In hepatic arteriovenous fistulae, anastomosis typically involves the portal vein and hepatic artery.[2,3,6,9,12] However, there are reports of involvement of the cystic artery in humans.[10] Microhepatia is commonly observed due to abnormal portal blood flow.

4

Portal hypertension may result in the development of numerous portocaval acquired shunts.

Histology of AV fistulae reveals mass-like proliferations of abnormal arteries and veins, with arterialization of veins. The internal elastic lamina is frequently fragmented, split, or duplicated; in both veins and arteries, the tunica intima is expanded by smooth muscle invasion and hypertrophy, increased deposition of elastin fibers, edema, and mucinous matrix. The tunica media of veins and arteries also exhibits smooth muscle hypertrophy. Additionally, fibrinoid necrosis may be observed. Elastin (Verhoeff-Van Gieson) and trichrome (Gomori's trichrome) stains highlight the deposition of elastin fibers and fiber fragmentation as well as the fibrosis that often accompanies the fistulae.[3,5,6] In fistulae that affect the liver, lesions resembling portocaval shunting occur, including absence or diminution of portal veins, marked biliary and arteriolar proliferation, hepatocyte atrophy, and lymphangiectasia.[2,3,6,9,12] Sinusoids near the fistulae are frequently dilated and congested. Liver lobes away from the fistulae may be normal with little parenchymal change.[3]
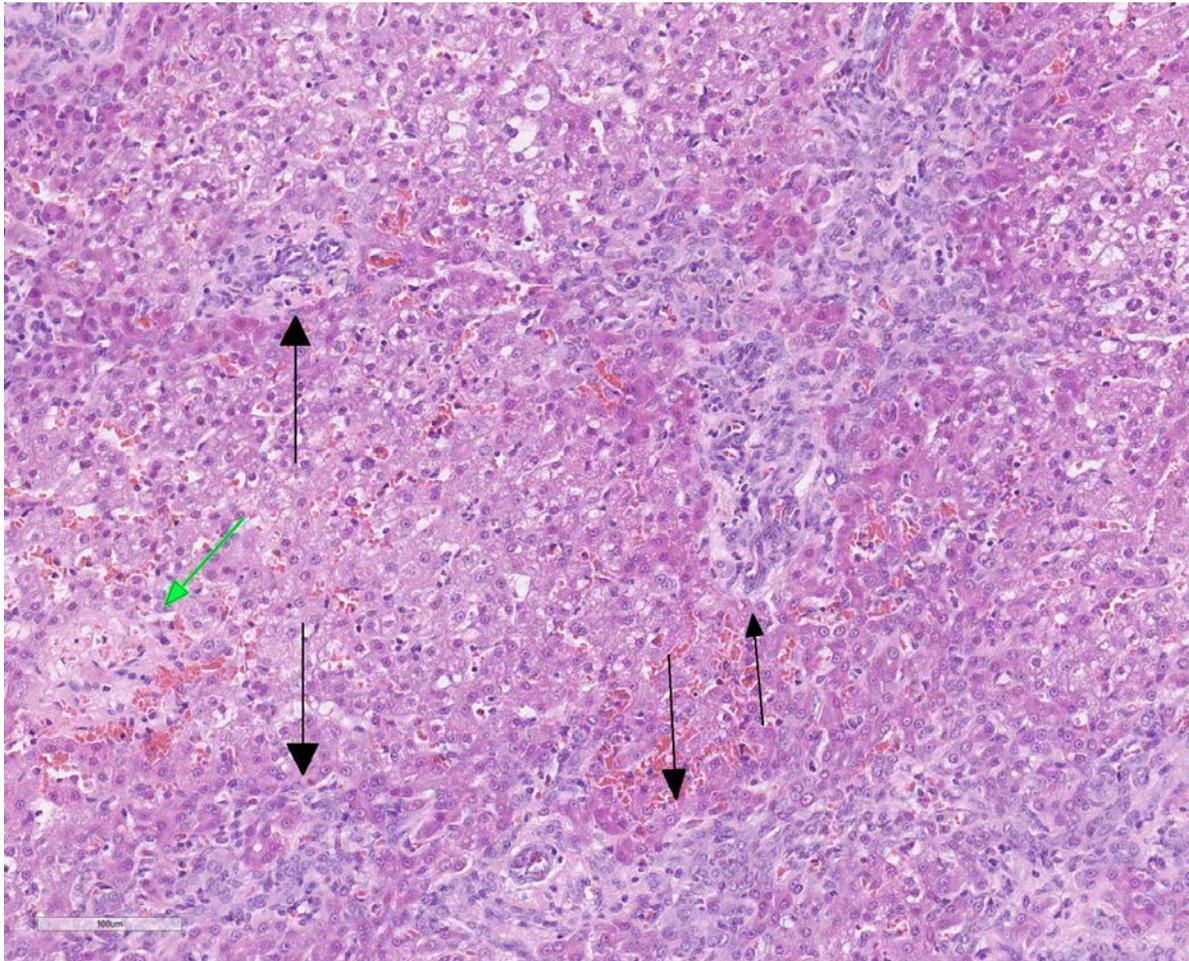
Liver, dog. At a distance from the arteriovenous fistula, portal triads are expanded by marked biliary hyperplasia and fibrosis (black arrows). There is hepatocellular necrosis and loss surrounding a central vein (green arrow).) (HE, 400X)

Treatment of AV fistulae is dependent upon location; advanced imaging such as ultrasonography, computed tomography, and magnetic resonance imaging can facilitate therapeutic intervention. Surgical excision, interventional techniques, and coil embolization have been described in a variety of cases.[5,8].

Contributing Institution:

North Carolina State University, College of Veterinary Medicine, Department of Population Health and Pathobiology
https://cvm.ncsu.edu/research/departments/dphp/

JPC Diagnosis: Liver: Aberrant arterial connection, focal, severe, with arterial and venous intimal and medial hyperplasia and fibroelastosis, hepatocellular atrophy, congestion, and hemorrhage.

JPC Comment: The contibutor has done an excellent and concise review of arteriovascular fistulae in the dog. Intrahepatic arteriovenous fistulae are most often acquired in humans as a result of surgical intervention, such as hepatic biopsy, transhepatic intervation such as percutaneous cholangiography, surgery or transplantation, and occasionally as a result of trauma. They may also arise within neoplasms (most commonly those which have an endothelial vasoproliferative component, such as infantile hemangiomas).[4]

In the dog, as in this case, they are likely congenital malformations that often result in portal hypertension as a result of the pressure differential between the hepatic artery and the low-pressure system of the portal circulation. In most affected dogs, large, pulsating vessels on the surface of one or more affected lobes are seen during surgery[6]; Doppler imaging is a commonly used imaging modality for diagnosis.[4,11] As mentioned by the contributor, microhepatia is a common finding in affected dogs, but the affected lobes are enlarged by the presence of the fistulae.[6] The WSAVA Liver Standardization group, in their 2006 tome, *Standards for Clinical and Histological Diagnosis of Canine and Feline Liver Diseases*, put forth their "strong impression" that arteriovenous fistulas are usually associated with portal vein hypoplasia, based on the observation that recovery from portal hypoperfusion has never been truly recorded following surgical resection of affected lobes.[11]

This particular case demonstrates the need for special stains for all microscropic evaluation of vascular lesions, and especially arteriovenous fistulae which have significant mural changes. On HE examination, the thickness of the arterial wall can be estimated, and gross disorder of smooth muscle cells can be identified, but much of the fine detail is obvious only after employment of various histochemical stains. A stain for elastin, such as Movat's pentachrome or Verhoeff-van Gieson, is imperative to identify fragmentation or loss of the internal elastic membrane. Loss of the internal elastic lamina allows migration of smooth muscle cells to the tunica interna, where they may dedifferentiate to a secretory phenotype and engage in arterial wall remodeling by synthesizing extracellular matrix components.[1] A stain for collagen, such as a Masson's trichrome, will demonstrate the amount of collagen within the remodeled intima; and a Movat's pentachrome will also demostrate excess intercellular elastin fragments as well.

The presence of two sections of liver, one containing sections of the fistula as well as one taken nearby, show significant

difference in degree of hepatocellular atrophy. While there is atrophy of hepatocytes in both sections (as is common in dogs with congenital and marked decreases in portal blood flow), there is significant hepatocellular loss in proximity to the fistulae, likely due to compression from the expanded vasculature as well. Examination of the portal triads in the section further away from the fistulae is informative as well, as portal areas contain numerous profiles of hepatic arterioles and bile ductules, but few visible profiles of portal veins. The marked siusoidal dilatation and hemorrhage is the result of the shunting of blood from the hepatic artery into the portal vein, and the generated pressure also results in dilation of lymphatics in both section, most prominently and strikingly around the sublobular veins (the so-called "rose window" effect, per personal communication, Dr. John Cullen.

The moderator adeptly summarized the changes in the slide by stating that "when you see arteries looking like veins and veins looking like arteries, you must add arteriovenous fistula or malformation to your differential diagnosis". The moderator noted another particular histologic finding in this section in the walls of hypertrophic arterioles – the apparent formation of two distinct layers of smooth muscle, oriented perpendicularly to each other – not a specific finding , but an indication of arterial wall disease.

The moderator opined that in the diagnosis of arteriovenous malformations, imagining is the gold standard, and hopefully the histology is supportive – diagnosis solely on histology may be problematic. The participants discussed the difference between arteriovenous "fistula" and "malformation". Arteriovenous fistulas are composed of a single connection between arteries and veins and the histologic findings may be more obvious on histology; artiovenous malformastions are multiple connections often formin a niduls of connections which may or many not be as easily discerned on histology.

Finally, the discusion of chronic congestion versus hemorrhage, which obscured much of the hepatic parenchyma on the slide was determined to be complicated by the fact that this sample was a biopsy.

References:

1.   Aiello VD, Gutierrez PS, Chaves MJF, Lopes AAB, Higuchi ML, Ramires JAF. Morphology of the Internal Elastic lamina in arteries from pulmonary hypertensive patients: a conocal laser microscopy study. *Mod Pathol* 2003; 16(5):411-416.
2.   Booler, H. Congenital Intrahepatic Vascular Anomaly in a Clinically Normal Laboratory Beagle. Tox Path. 2008, 36: 981-984
3.   Cullen, JC and Stalker, MJ. Liver and Biliary system. In: Maxie MG, ed. *Jubb, Kennedy, and Palmer's Pathology of Domestic Animals*. Vol 2. 4th Edition. St. Louis, MO: Elsevier; 2016. 266.
4.   Gallego C, Miralles M, Marin C, Muyor P, Gonzalez G, Garcia-Hidalgo E. Congenital hepatic shunts. *RadioGraphics* 2004; 24:755-772.
5.   Leach, S.B., Fine, DM., Schutrumph, RJ., Britt, LG., Durham, HE., Christiansen, K. Coil embolization of an aorticopulmonary fistula in a dog. J Vet Cardiol. 2010; 12: 211-216.
6.   Moore, P. F. and Whiting, P. G. Hepatic lesions associated with intrahepatic arterioportal fistulae in dogs. Vet Path. 1986; 23 (1): 57-62.

7.   Robinson, WF and Robinson, NA. Cardiovascular system. In: Maxie MG, ed. *Jubb, Kennedy, and Palmer's Pathology of Domestic Animals*. Vol 2. 4th Edition. St. Louis, MO: Elsevier; 2016. 56.

8.   Saunders, AB., Fabrick, C., Achen, SE., Miller, MW. Coil embolization of a congenital arteriovenous fistula of the saphenous artery in a dog. J Vet Intern Med. 2009; 23: 664-664.

9.   Schaeffer, IGF., et al. Hepatic arteriovenous fistulae and portal vein hypoplasia in a Labrador retriever. JSAP. 2001; 42: 146-150.

10.   Tajima, H., Hosaka, J., Tajma, N., Kumazaki, T. Arteriovenous malformation of the gallbladder. Eur. Radiol. 1997; 7: 333-334.

11.   Rothuizen J, Bunch SE, Charles JA, Cullen JM, Desmet VJ, Szatmari V, Twedt DC, van den Ingh TSGAM, Ven Winkle T, Washabau RJ. Morphological classification of circulatory disorders of the canine and feline liver. . *In:* WSAVA Standards for Cinical and Histological Diagnosi of Canine and Feine Liver Disease.   Edinburgh, Saunders-Elsevier, 2006, pp 53-55.

12.   Yoshizawa, K., Oishi, Y., Matsumoto, M., Fukuhara, Y., Makino, N., Noto, T. Fujii, T. Congenital Intrahepatic arteriovenous fistulae in a young beagle dog. Tox Path. 1997; 25: 495-499.

CASE II: 17/1060 Z (JPC 4032584).

Signalment: 4 year old, female spayed, Bull Arab (canine)

History: Sudden death. The week before death, the animal was showing signs of hind limb/spinal pain. Radiographs at that time revealed a sublumbar mass and fluid in the caudal abdomen, fluid PCV/TP 15/70.

Gross Pathology: Abdominal cavity: The abdomen contains approximately 1300 ml of dark red, slightly turbid fluid (blood) admixed with tens of variably sized, friable, soft dark red material (blood clots). The dorsocaudal abdomen, ventral to lumbar vertebrae 6 and 7 and the iliopsoas muscles, contains a poorly demarcated, approximately 11 x 5 x 4 cm, firm mass which surrounds and replaces approximately 7 cm of the aorta. On cut section, the mass is mottled dark pink to dark red and cavitated. The caudal aspect of the mass is friable with roughened edges and contains approximately 10 ml of clotted blood (site of rupture).

Spleen: The tail of the spleen contains a focal, poorly demarcated, approximately 1cm in diameter, raised, irregular, soft mass, which is mottled dark red to tan on cut surface.

Kidney: The medulla of the right kidney contains a focal, 0.9 x 0.5 x 0.4 cm depressed area, which contains less than 1
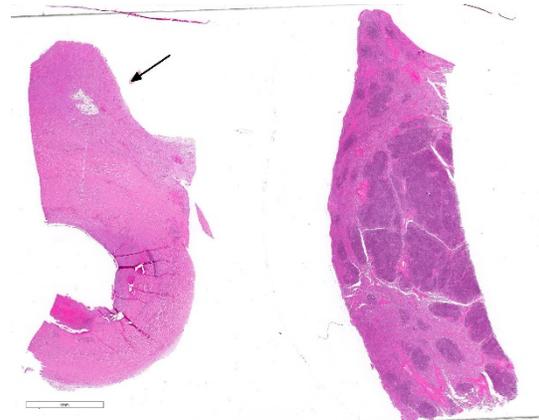
Aorta and spleen, dog. The wall of the aorta (left) is markedly thickened and fibrous connective tissue partially effaces the adventitial adipose tissue (arrow.) Areas of hypercellularity are evident in the aortic wall. Large areas of hypercellularity coalesce within the splenic parenchyma (right). (HE, 7X)

ml of turbid, mucoid, viscous, yellow fluid (granuloma).

Gross morphological diagnoses:

Abdominal cavity: Aortic arteritis, aneurysm with rupture and haemoabdomen

Spleen: Granulomatous Splenitis, focal, moderate, chronic

Kidney: Granulomatous nephritis, focal, moderate, chronic

**Laboratory results:**

Fungal culture:

Spleen: Very small fungal colonies isolated following 48 hours incubation. Growth identified as *Aspergillus terreus*

Microscopic Description:

Aortic mass**:** Generally, approximately 20% of the aorta is expanded up to three-fold with inflammation, necrosis and haemorrhage. The tunica intima, and to a lesser extent, the tunica media, contain multifocal to coalescing areas of dense
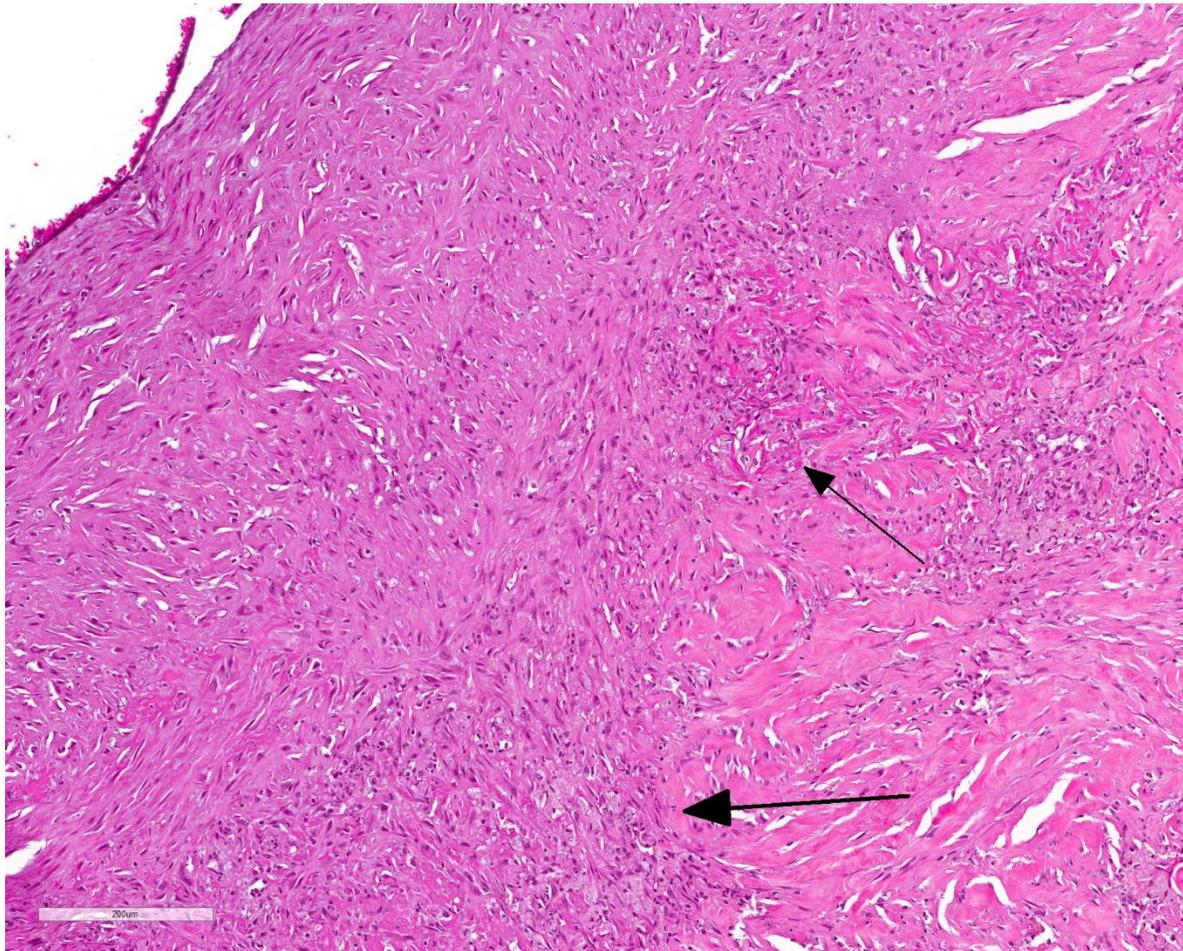
Aorta, dog. The tunica intima is effaced by migration of smooth muscle cells, fibrous connective tissue and elastin, and blends with the underlying tunica media. Within the media there is a dissection which is surrounded by neutrophils, eosinophils, and macrophages (arrows). (HE, 131X)
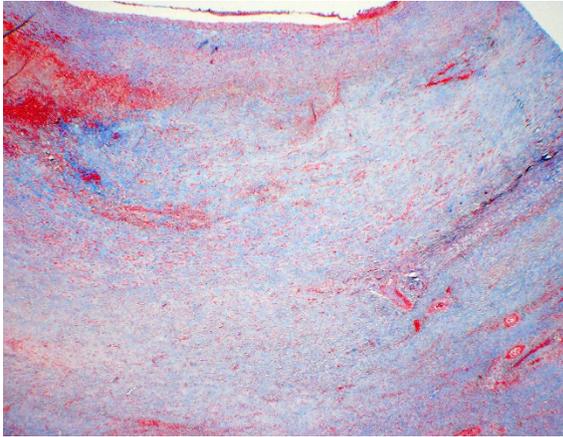
A Masson's trichrome demonstrates the tremendous amount of collagen that expands the wall of the aorta (arrows). The edge of the dissection the red area at upper left. (Masson's trichrome, 40X)

of eosinophilic fibrillary material (fibrin). Macrophages are often epithelioid or forming multinucleated giant cells which engulf or surround hundreds of 3-5 micron-thick, 5-100 micron-long, branching fungal hyphae which are septate with conidial heads and are GMS positive. The tunica media contains large, up to 2000 micron in diameter lakes of extravasated erythrocytes (haemorrhage) admixed with degenerate neutrophils, hyperoesinophilic material, pyknotic and karyorrhectic debris (necrosis). No bacteria are observed on gram stain.

Spleen: In approximately 60% of the tissue section, the white and red pulp are completely effaced by dense infiltrates of lymphocytes and plasma cells which surround hundreds of multifocal with moderate numbers of fungal organisms as described for the aortic mass. The remaining parenchyma contains a reduction in lymphocytes density (depletion) with increased numbers of randomly scattered neutrophils admixed with necrotic debris. aggregates of macrophages, multinucleated giant cells and lesser numbers of neutrophils.

aggregates of degenerate neutrophils and macrophages admixed with large amounts

Macrophages and giant cells often contain or are associated

Contributor's Morphologic Diagnosis:

Aortic mass: Necrotising granulomatous arteritis, severe, generalised, chronic with fungal hyphae (morphology consistent with *Aspergillus terreus*).

Spleen: Granulomatous splenitis, focal, severe, chronic with intralesional fungal hyphae

Contributor's Comment: Aortic aneurysm is a localised dilation of the vessel which may occur secondary to loss of vessel wall integrity. Aneurysms are rare in domestic animals, and may occur secondary to atherosclerosis, medial degeneration, trauma, infection or arterial dissection.[5] In this animal, large amounts of necrosis and inflammation which contain fungal organisms are consistent with a mycotic aneurysm. In this case, the infection has caused a weakening of the vessel wall and
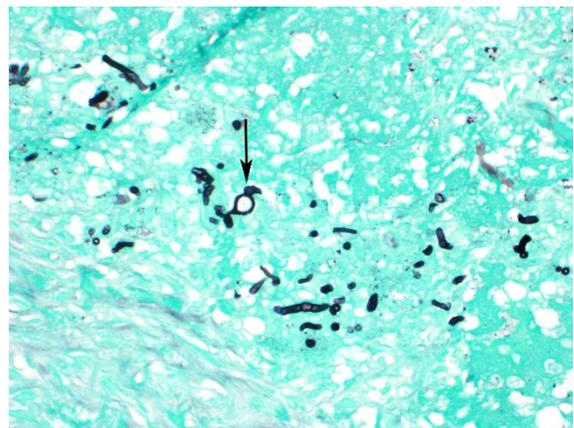
Aorta, dog. A GMS stain demonstrates fungal hyphae in areas of mural necrosis – the hyphae are septate, with parallel walls, and occasionally globose chlamydospore-like swellings (arrow). (HE, 131X)

subsequent rupture, leading to sudden death from acute and massive haemorrhage into the abdomen.

Aspergilli are ubiquitous and can be isolated from soil, air and decomposing organic matter. Infection is acquired from environmental sources, generally by inhalation or ingestion. It is an opportunistic pathogen depending on impaired, overwhelmed or bypassed host defences. Infection may cause local disease, or disseminate to other parts of the body. Evidence of infection and inflammation within the spleen and kidney in this animal is consistent with

disseminated disease; however, the original route of infection is undetermined.

Fungal aortic aneurysms have been reported twice previously in dogs.[1,3] In one case, *Graphium* species was isolated from the aneurysm, and *Candida* infection was suspected in the second. In humans, *Aspergillus* species are the most common mycotic infections associated with aneurysms.

A variety of risk factors may be associated with the development of these infections.[1] Reported risk factors in humans include broad-spectrum antibiotic use, mechanical ventilation, parenteral nutrition, renal
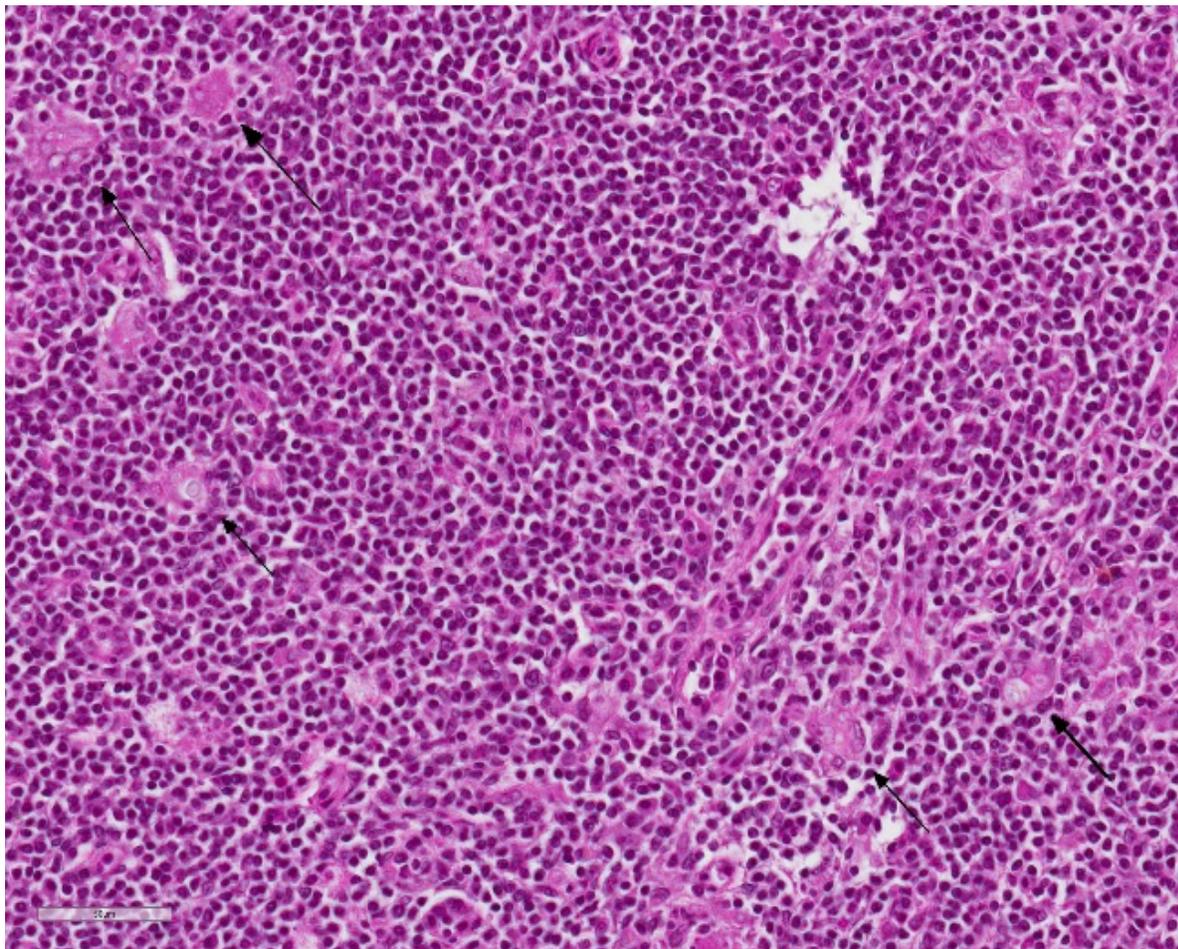
Spleen, dog. there are scattered multinucleated giant cell macrophages which often contain negative outlines of fungal hyphae (arrows)   (HE, 400X)
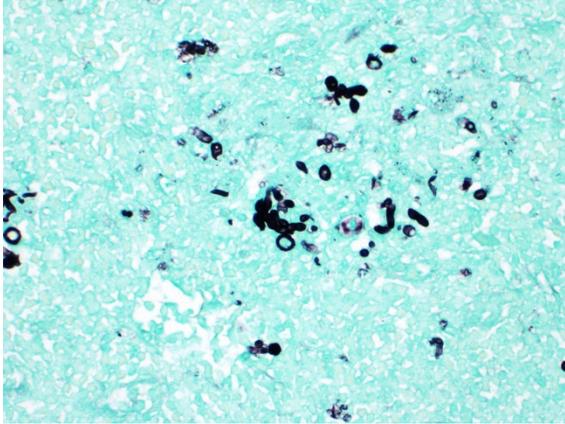
Spleen, dog. A GMS stain demonstrates clusters of fungal hyphae in the spleen. (HE, 400X)

failure, prior surgery, neutropenia, chemotherapy, severe illness, age, and indwelling catheters (especially central venous catheters). Although less commonly reported, veterinary patients appear to have similar risk factors. In one of the case studies cited, however, no predisposing factors were able to be identified.

JPC Diagnosis: 1. Aorta: Elastolysis and fibrosis, transmural, diffuse, severe, with vascularization and dissection.

2. Aorta: Aortitis, pyogranulomatous, focally extensive, severe, with transmural fibrosis and numerous fungal hyphae.

3. Spleen: Splenitis, granulomatous, diffuse, marked with numerous fungal hyphae and lymphoid depletion.

JPC Comment: A caution - the term "mycotic aneurysm" (which may be found repeatedly in Pubmed) is itself a misnomer, as this term, coined by Osler in 1885, refers to a focal aneurysm of an arterial wall due to any infectious cause, not just a fungal one.[6] The term, as applied by Osler, was used to describe the "mushrooming" appearance of the lesion, rather than any particular fungal

origin. Most cases of infectious aortitis are the result of opportunistic bacterial infections of pre-existing lesions.

True fungal infections of the aorta are uncommon in all species. They are most commonly dommented in humans, where the may be the result of mycotic infection from other sites (especially in immunocompromised individuals) as well as seen as a devastating complication from a variety of surgical interventions as a result of improper sterilization, including valvular replacement surgery, aortocoronary bypass, and aortic segment replacement.[8]

Documented manifestations of aortic aspergillosis include ascending aortic pseudoaneurysm ansd aspergilloma with supravalvular aortic stenosis.[10] Reports of mycotic aneurysms in animals are even less common. A previous report of *Basidiobolus* infection in a sooty mangabey was published[7] shortly prior to its usage in the Wednesday Slide Conference (WSC Conf. 4, Case 1). The animal was found dead with no premonitory sign following spontaneous rupture of the aneurysm.[7] Aortic aneurysms are well-known in horses and groundhogs[9], both verminous and spontaneous, but only one report of an aortic aneurysm arising from a fungal agent exists.[4]

Few reports of aortic aneurysms due to *Aspergillus terreus* exist for any species (including humans); approximately 90% of reports are the result of infection with *A. fumigatus. A terreus* species complex infections are about 4%.[2] Two cases of aortic aneurysm as a result of *A. terreus* infection have been reported, both arising in sites of previous surgery in patients undergoing cancer chemotherapy.[8]

The most common pathogenic species of *Aspergillus* include the members of the *A. fumigatus* species complex, the *A. flaus* species complex, the *A. niger* species

12

complex, and the *A. terreus* species complex. The *A. terreus* species complex is composed of 16 related species which are found worldwide. They are common soil-borne fungi which can be found in arable soil, compost, and even deserts. They produce light-brown colonies on Sabouraud agar, with characteristic lateral aleurioconidia which attach directly to hyphae. It is used in the pharmaceutical industry to produce lovastatin. [2]

In humans, most *A. terreus* infections are seen in immunocompromised hosts, but chronic pulmonary disease may also be a precipitating factor.[2] In animal species, *A. terreus* has been well documented as a cause of disseminated aspergillosis in the dog,[1,5] with German Shepherd dogs being overrepresented. Breed-associated abnormalities in IgA levels have been postulated as a cause, but not definitively proven. Granulomatous inflamation with fungal hyphae is seen in a number of organs; renal involvement is common (seen in this case, but not submitted) as is myocardial involvement.[1,5] *Aspergillus terreus* is known for a resistance to amphotericin B; 98% of clinical isolates in humans demonstrate a resistance to the drug.[2,8] Luckily, it is the species of *Aspergillus* most susceptible to itraconazone and related antifungals.[2,8]

The moderator noted the presence of vessels within the wall of the aorta – as this is a section of abdominal aorta which should normally be avascular. As a general rule, the walls elastic arteries of small and laboratory animals should not have vasa vasorum; those of ruminants and horses do. The moderator said that he suspected the aneurysm to be the pre-existent lesion and the fungal infection to be secondary.

References:

1. Gershenson RT, et al. Abdominal Aortic Aneurysm Associated with Systemic Fungal Infection in a German Shepherd Dog. *J Am Anim Hosp Assoc.* 2011;47(1):45-49.

2. Lass-Florl, C. Treatment of infections due to *Aspergillus terreus* species complex. *J Fungi* 2018: 4:83-92.

3. Murata Y, et al. Mycotic aneurysm caused by Graphium species in a dog. *J Vet Med Sci.* 2015; 77(10):1285-1288.

4. Okamoto M, Kamitani M, Tunoda N, Tagami M, Nagamine N, Kawata K, Itoh H, Kawasako K, Komine M, Akihara Y, Shimoyama Y, Miyasho T, Hirayama K, Kikuchi N, Taniyama H. Mycotic aneurysm in the aortic arch of a horse associated with invasive aspergillosis. *Vet Rec* 2007; 160:268-270.

5. Robinson WF and Robinson NA. Cardiovascular system. In: Grant Maxie M, ed. *Jubb, Kennedy and Palmer's Pathology of Domestic Animals.* vol 3, 6th ed. Elsevier, Missouri. 2016:68-69.

6. Salzberger LA, Cavuoti D, Barnard J. Fatal *Salmonella* aortitis with mycotic aneurysm rupture. *Am J Forens Med Path* 2002; 23(4):382-385.

7. Sharma P, Cohen JK, Lockhart SR, Hurst SF, Drew CP. Ruptured mycotic aortic aneurysm in a sooty mangabey (*Cercocebus atys*).

8. Silva ME, Malagolowkin MH, Hall TR, Sadeghi AM, Krogstad P.

Mycotic aneurysm of the thoracic aorta due to *Aspergillus terreus*: case report and review. *Clin Inf Dise* 200; 31:1144-1148.

9. Snyder RL Ratcliffe HL. *Marmota monax*: a model for studies of cardiovascular, cerebrovascular and neoplastic disease. *Acta Zool Pathol Antvep* 1969; 48:256-273

10. Watanabe, I, Nakayama T, Yamada E, Tsukino M, Hayashi E. Invasive aspergillosis in the aortic arch with infectious *Aspergillus* lesions in pulmonary bullae. *Med Mycol Case Rep* 2015; 7:15-19.

10.

CASE III: WSC Case 1 (JPC 4049886).

Signalment: 22Y 6M 12D, female, common squirrel monkey (*Saimiri sciureus*).

History: Patient was found dead in its enclosure. Patient had been exhibiting abnormal behavior the day prior. A necropsy was performed and tissue specimens were submitted in formalin for histopathologic evaluation.

Gross Pathology: There were multiple, multifocal, up to 1 mm diameter dark red-black foci throughout the cerebral gray matter. A small amount of bruising and emorrhage was noted in the rostral mandible.

Laboratory Results (clinical pathology, microbiology, PCR, ELISA, etc.)**:** None.

Microscopic Description: Diffusely, cerebral meningeal and parenchymal vessels are transmurally expanded and effaced by variable amounts of amorphous, finely fibrillar to waxy, pale eosinophilic material (amyloid). Multifocally, affected vessels are surrounded by mild to moderate amounts of fibrinoid exudate and acute to chronic hemorrhage as well as mild to moderate numbers of gitter cells that occasionally contain golden-brown globular intracytoplasmic pigment (hemosiderin), lymphocytes and plasma cells and fewer gemistocytic astrocytes and occasional multinucleate giant cells. There are multifocal small (10-25 um) round parenchymal deposits (senile plaques) often adjacent to affected vessels.

Contributor's Morphologic Diagnosis:

Cerebrum, vessels: Amyloidosis, transmural, diffuse, severe, with hemorrhage, fibrinoid exudation, astrogliosis, senile plaques and occasional multinucleate giant cells.

Contributor's Comment:

 The histomorphologic findings in the cerebrum are consistent with cerebral amyloid angiopathy (CAA) – a vascular disorder caused by the accumulation of amyloidogenic proteins in the walls of cerebral blood vessels.[4] In severe cases, CAA can result in other vasculopathic changes such as microhemorrhages, fibrinoid extravasation and focal gliosis.[4] In some cases, vascular/perivascular inflammation, fibrinoid necrosis and leukoencephalopathy have been associated with vascular β-amyloid deposition.[4] The

predilection to developing age-related CAA has been confirmed in the squirrel monkey and they are an animal model for CAA in humans, in whom it has been shown to increase the risk of intracerebral bleeding and has been associated with up to 20% of non-traumatic hemorrhagic strokes in the elderly.[4] Additionally, CAA is a risk factor for cognitive decline (even in the absence of stroke) and may worsen the dementia of Alzheimer's disease (AD).[4] Currently, there are no practical antemortem diagnostic tests or treatments for CAA. CAA-related vasculopathies arise in squirrel monkeys but are not common. In severely affected animals (as in this case), microhemorrhages and fibrinoid exudation may occur. Several studies support squirrel monkeys as an optimal biological model for idiopathic CAA and for testing the safety and efficacy of β-amyloid reduction strategies such as β-amyloid-immunization therapy for AD.[4]

The pathogenesis of CAA remains obscure; however, failure of active/passive elimination of β-amyloid from the aging brain may play an important role.[4] Squirrel monkeys naturally develop β-amyloid deposits in the form of CAA and senile plaques starting at approximately 13 years of age.[4] Their life span in captivity is up to 30 years. Additionally, their cerebrovascular and immune systems are similar to humans. The β-amyloid precursor protein in squirrel monkeys is 99.5% homologous to human βAPP751 and the amino acid sequence of β-amyloid is identical in the two species.[2] Severely affected arterioles show loss of smooth muscle cells in the tunica media leading to weakening of the vascular wall and an increased propensity to rupture,
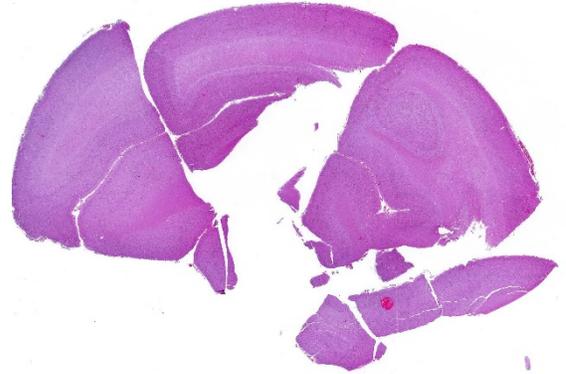
Cerebrum, squirrel monkey. Fragments of cerebrum are presented for examination. A subgross magnification, no lesions are visible, save for a focal area of hemorrhage at lower right. (HE 6X).

leading to intracerebral bleeding.[2] Amyloid accumulation in cerebral vessels is known to induce degeneration of the entire neurovascular unit. Not only does the accumulation of insoluble amyloid species in vascular walls cause alterations of smooth muscle and endothelial cell layers, but amyloid deposition and concomitant microhemorrhages also occur in capillaries lacking the smooth muscle layer.[5] Complement activation products co-localize with cerebral parenchymal and vascular deposits in AD and non-β-amyloid amyloidosis indicating that the chronic inflammatory response, most likely initiated by the deposits, is a general phenomenon.[5] Once complement components are generated, they participate in several key steps of amyloidogenesis (aggregation, microglial activation and phagocytosis).[5] Other markers of inflammation in AD include elevated cytokines and chemokines as well as accumulation of activated cytokine-expressing microglia found in or near pathologic lesions.[5]

Capillaries are especially vulnerable to CAA in squirrel monkeys,[4] while in humans,
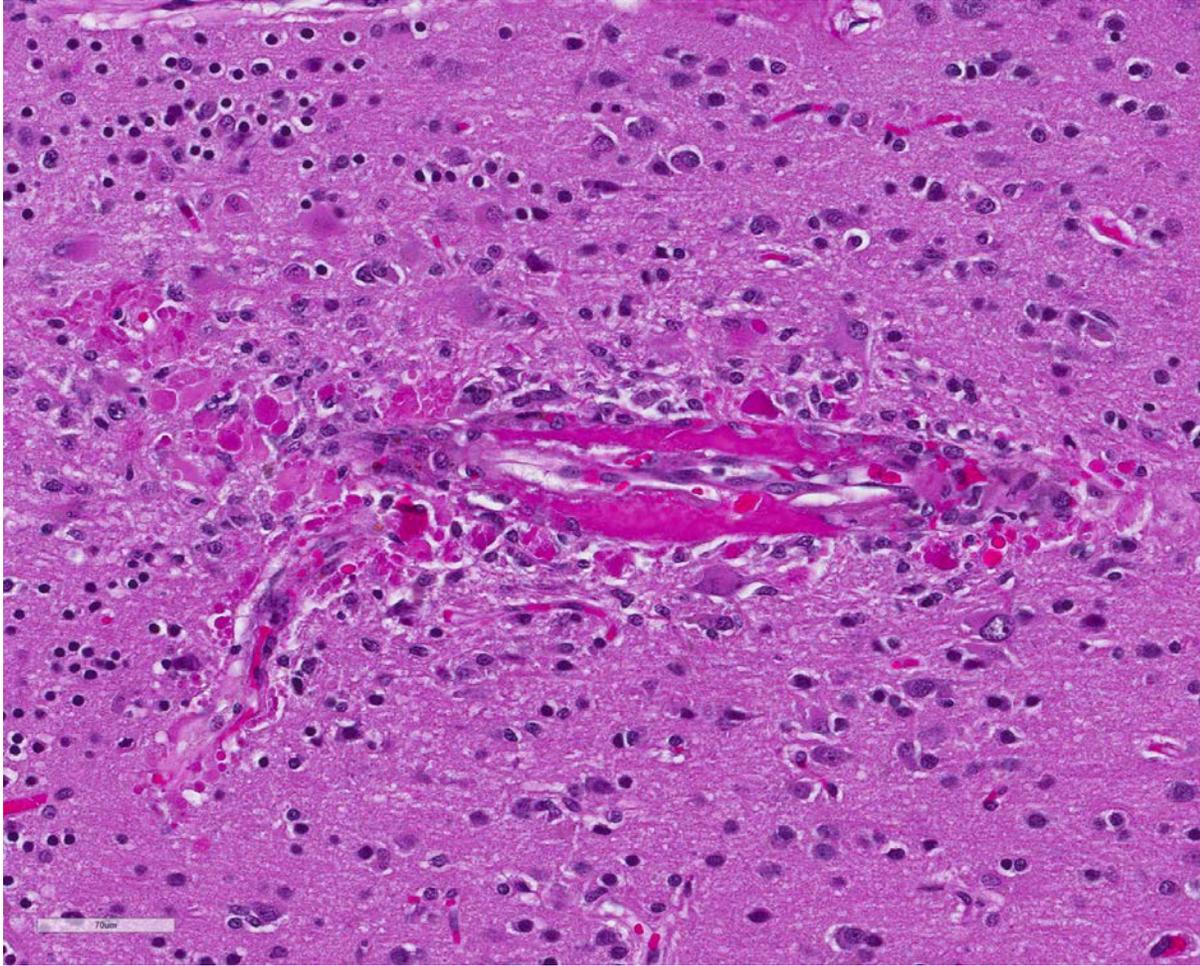
Cerebrum, squirrel monkey. Parenchymal vessel walls are expanded by brightly eosinophilic amyloid and surrounded by macrophages, astrocytes, and globules of extruded protein. (HE 6X).

leptomeningeal and cortical arteries and arterioles are especially vulnerable. Both (vessels and parenchyma) types of β-amyloid deposits occur primarily in the neocortex with the highest density of lesions in the rostral cortex, diminishing caudally.[4] Distribution and quantity of deposits are highly symmetrical in the right and left hemispheres.[2] In the squirrel monkey, aggregated β-amyloid occupies meningeal and parenchymal arteries/arterioles as well as numerous parenchymal capillaries.[4] Few capillaries are congophilic and, as in humans, veins are seldom amyloidotic.[4] In

the arteriolar wall, the basal lamina of the tunica media is the primary site of β-amyloid accumulation.[4] The tunica adventitia is also frequently involved.[4] When severe, there is effacement of hypocellularity of the vascular wall – especially within the tunica media.[4] In contrast to humans, large parenchymal senile plaques are relatively infrequent in aged squirrel monkeys and when they occur they are usually small (10-25 um in diameter) and spherical.[4] Amyloidotic vessels occasionally may be surrounded by

reactive microglia; however, they are more often associated with reactive astrocytes.[4]

CAA is ultrastructurally composed of classic amyloid fibrils and is the principal type of cerebral β-amyloidosis in squirrel monkeys.[4] The basal lamina of amyloidotic vessels is enlarged and distended by masses of classic amyloid fibrils. In capillaries, β-amyloid accumulates in the basal lamina and tunica adventitia (due to lack of tunica media proper). In some cases, β-amyloid in parenchymal and vascular lesions is coextensive.[4] Additional diagnostic tests include Congo Red special histochemical stain, β-amyloid immunohistochemistry, Thioflavin T fluorescent stain and the

Shtrasburg method. CAA has also been reported in a sooty mangabey.[5] This case was reviewed in consultation with Dr. Derek Mathis, MD neuropathologist.

Contributing Institution:

http://www.wpafb.af.mil/AFRL

JPC Diagnosis: Cerebrum, small and medium-caliber arteries: Amyloidosis , multifocal, moderate, with multifocal fibrinoid necrosis, and minimal perivascular granulomatous inflammation.

JPC Comment: The contibutor has done an excellent job in describing the syndrome of cerebrovascular amyloidosis (cerebral amyloid angiopathy – CAA) in the squirrel
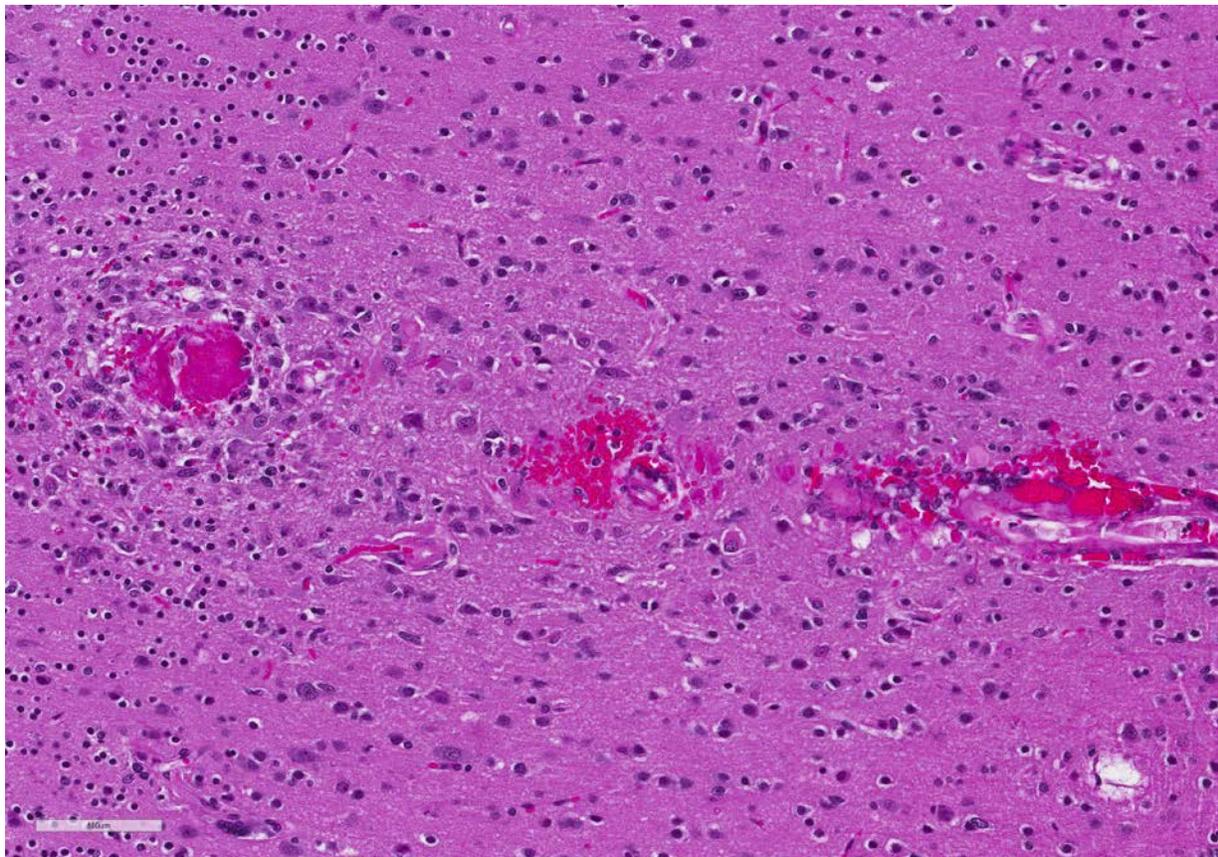
Macrophages, glial cells and rare gemistocytic astrocytes surround remnants of a thrombosed vessel (left). The walls of nearby vessels are expanded with amyloid and there is focal hemorrhage. There is gliosis of the surrounding parenchyma. (HE 254X).

monkey, perhaps the best animal model for a significant health problems in aging humans. Increasingly sophisticated imaging technologies are available today for antemortem detection CAA in squirrel monkeys. Magnetic resonance imaging has detected two distinct patterns associated with cerebrovascular amyloid – amyloid-related imaging abnormalities (ARIA). T-2 weighted MRI has identified an edematous type (ARIA-E), that appears as a hyperintense signal, and a hemosiderotic type (ARIA-H) which demonstrates a hypointense signal. The ARIA-E type demonstrates astrocytic and microglial hypertrophy in the white and grey matter.[6]

In humans, β-amyloid peptide (Aβ) is an integral part (along with tauopathy) in the development of Alzheimer's disease, and the misfolding of Aβ is considered the initiating event in the development of Alzheimer's disease (AD).[6] On its own, it is not associated with dementia or neurodegeneration in humans[6], but is considered a major cause of spontaneous intracerebral hemorrhage.[1]

CAA is commonly seen in elderly humans, and advancing age is the strongest risk factor for its development.[1] (Another risk factor, shared with AD, is the apoliporotein E (ApoE) epsilon IV (e4) allele).[4] Up to 40% of non-demented and 60% of demented individuals between the ages of 80 and 90 years may demonstrate CAA at autopsy.[1] One study suggests that it may be seen in up to 95% of humans with dementia if looked for diligently. A number of manifestations of CAA in humans in the absence of Alzheimer's disease have been described, to include spontaenous cortical hemorrhage (with associated microbleeds and siderosis), post-hemorrhage cognitive impairment, and transient focal neurological episodes ("amyloid spells").[1] A recent study

demonstrated significant cortical thinning in individuals with CAA.[3]

As mentioned above in context with the spider monkey, the currently accepted pathogenesis for CAA is not overproduction of Aβ, but deficiencies in clearance. Excess interstitial fluid in the brain is drained along arteries in the brain, bolstered by the pulsation of these vessels. The predominant theory of deposition is that as this perivascular drainage system fails with age, Aβ is progressive trapped in the expanding perivascular compartment, which allows for aggregation and deposition along vascular basement membranes.[1]

Regarding the comparative pathology of CAA, in addition to the squirrel monkey, there are a number of mouse models which overexpress Aβ and develop senile plaues and CAA, but no significant neurodegeneration.[7] A number of researchers have suggested species-specific differences in post-translational characteristics and the the formation of species-specific Aβ isoforms as a potential reason for the lack of associated neurodegenerative disease in some species. Squirrel monkeys also manifest extensive Aβ deposition, but not the additional lesions associated with Alzheimer's disease.[7]

The concurrent presence of amyloidosis and fibrinoid necrosis was interesting in this case. The moderator described histologic differences in the two which are best appreciated without the use of a condenser. In addition, the moderator demonstrated the presence of giant cells adjacent to arteries containing mural amyloid, as well as the discontinuity of arterial walls when stained with smooth muscle actin (most appreciable on arteries cut on longitudinal section.)

References:

1. Charidimou A, Boulouis G, Gurol ME, Ayata C, Bacskai, Frosch MP, Viswanathan A, Greenberg. Emerging concepts in sporadic cerebral amyloid angiopathy. *Brain* 2017; 140:1829-1850.
2. D'Angelo OM, Dooyema J, Courtney C, Walker LC and Heuer E. Cerebral amyloid angiopathy in an aged sooty mangabey (Cercocebus atys). Comp Med (2013) 63(6): 515-520.
3. DeSimone CV, Graff-Radford J, El-Harasis MA, Rabinstein AA, Asirvatham SJ, Homes DR. Cerebral amyloid angiopathy: diagnosis, clinical implications, and management strategies in atrial fibrillation. *J Am College Cardiol* 2017; 70(6):1173-1181.
4. Elfenbein HA, Rosen RF, Stephens SL, Switzer RC, Smith Y, Pare J, Mehta PD, Warzok R and Walker LC. Cerebral β-amyloid angiopathy in aged squirrel monkeys. *Histol Histopathol* (2007) 22:155-167.
5. Ghiso J, Fossati S and Rostagno A. Amyloidosis Associated with Cerebral Amyloid Angiopathy: Cell Signaling Pathways Elicited in Cerebral Endothelial Cells. *J Alzheimers Dis* (2014).
6. Heuer E, , Jacobs J, Du R, Wang S, Kiefer OP, Cintron AF, Dooyemy J, Meng Y, Zhang X, Walker L. Amyloid related imaging abnormalities (ARIA) in an aged squirrel monkey with cerebral amyloid angiopathy. *J Alzheimers Dis* 2017; 57(2): 519-530.
7. Rosen RF, Tomidokoro Y, Farberg AS, Dooyema, Ciliax B, Preuss Tm, Neubert, TA, Ghiso JA, LeVine H, Walker LC. Comparative pathobiology of Aβ and the unique susceptibility of humans to Alzheimer's disease. *Neurobiol Aging* 2016; 44:185-196.

CASE IV: 21465 (JPC 4135536).

Signalment: 18 month old male Bassett hound (*Canis lupus familiaris*)

History: Mild ataxia, with cardiac enlargement of uncertain origin.

Gross Pathology: The dog has body weight of 17.0 kg. Watery joint fluid, with synovial hyperplasia, is present in several larger joints, but is particularly marked in the left coxofemoral joint. The subcutaneous fascia is thicker than expected over the muscles of the rear limbs, with reduced adipose tissue. The corneas are bilaterally cloudy. Thick dense spongy bone was present in cross-sections of the anterior calvarium. The
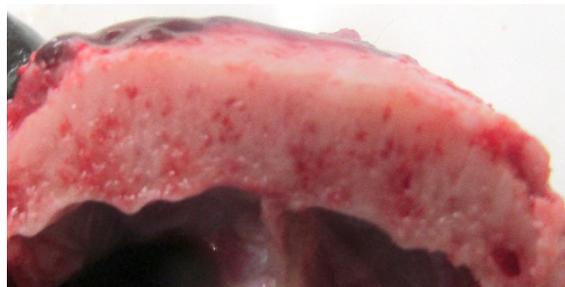
Calvarium, dog. Cross-section of bone of the anterior calvarium, showing increased width are reduced spongy texture. (Photo courtesy of: Veterinary Medical Diagnostic Laboratory, University of Missouri, 610 East Campus Loop, Columbia MO 65211, http://vmdl.missouri.edu/; http://vpbio.missouri.edu/)

Ribs, dog. Pleural aspect of the right costochondral junction, showing spatulate ribs. (Photo courtesy of: Veterinary Medical Diagnostic Laboratory, University of Missouri, 610 East Campus Loop, Columbia MO 65211, http://vmdl.missouri.edu/; http://vpbio.missouri.edu/)

costochondral junctions of the ribs are mildly offset, with a spatulate form. The skeletal muscles are pale, especially masseters and maxillary muscles. Both interventricular heart valves are extensively and irregularly somewhat irregularly, but have, rounded, smooth surfaces, and a gelatinous texture. Associated chordae tendonae are pearly white.

Laboratory Results: A mutation was found in the α-L iduronase gene by PCR.

Microscopic Description: Submitted tissues consist of thoracic aorta and heart with muscular arteries in the epicardial fat.

The elastic aortic wall is has elevated, plaque-like thickenings in the intima that bulge into the lumen, but remain covered by a single layer of flat endothelium. In the media, smooth muscle cells have a regimented appearance, and are separated into stacks by elastic fibers and increased interstitial ground substance with H&E (Fig. 5). Medial myocytes are diffusely contain unstained, well-defined cytoplasmic vacuoles. Despite this generally well-organized microanatomy, there is multifocal disorganization of the wall, a band of vacuolated macrophages located in the intima and inner media (Fig. 6), multifocal medial vacuolation around the vasa vasorum (Fig 7). These areas contain a multitude of foamy macrophages that form disorganized islands in the superficial wall and contribute to the substance of the plaques. Similar vacuoles occur in the muscularis of muscular arteries in the epicardial fat (Fig. 8) with disorganization of the vascular wall. The adventitia of these arteries contains increased ground substance and vacuolated macrophages in both muscularis and adventitia. There is very mild increase in lipofuscin on either side of cardiomyocyte nuclei sectioned longitudinally (not shown).

Movat's pentachrome staining was used to differential stain to determine the stromal components of the plaques (Fig.9). This stain produces black staining of elastin, while mucopolysaccharides stain green, collagen yellow, and muscle stains red. Small elastin fibers of the tunica intima is disorganized, and the plaque is easily demarcated from the internal elastic lamina of the media. Myocytes are outlined by elastin as well. The plaque is less intensely stained green, detecting mucopolysaccharides in its ground

Tricuspid valve. Valve leaflets are enlarged. (Photo courtesy of: Veterinary Medical Diagnostic Laboratory, University of Missouri, 610 East Campus Loop, Columbia MO 65211, http://vmdl.missouri.edu/; http://vpbio.missouri.edu/)

substance. Elastin staining is less organized in the intimal plaque and around the vasa vasorum. With Alcian blue-PAS 1.0 and 2.5, blue staining of sulfomucins predominated between the medial myocytes (Fig 10), but cytoplasmic vacuoles are shaded in pink along the edges (neutral and carboxymucins mucins). Vacuoles are found within muscle cells of the epicardial arteries.

Laboratory Results (clinical pathology, microbiology, PCR, ELISA, etc.)**:**

A mutation was found in the α-L iduronase gene by PCR.

Contributor's Morphologic Diagnosis:

Arteriopathy, with aortic plaques and stromal dysplasia, consistent with mucopolysaccharidosis

Contributor's Comment:

As a group, the mucopolysaccharidoses result from defective glycosaminoglycan catabolism. [9, 10] They are characterized by accumulation of glycoaminoglycans (GAG) in lysosomes. The most severe form, a deficiency of α-L iduronidase, causes Hurler's syndrome (MPSI), and results in increased retention of both dermatan sulfate and heparin sulfate in cells and interstitium.[9] Both metabolites are shed in urine of patients. Failure to hydrolyze these two substrates results in their accumulation in lysosomes, triggering complex of intracellular events leading to clinical signs that are directly linked to mechanical consequences of GAG storage.[5] Common findings in humans include laryngeal and tracheal narrowing, hearing and visual deficits, gargoyle faces, skeletal deformities, and heart valve disease with cardiomyopathy due to cardiac rigidity.[9,10]

Over 100 enzyme defects have been described in people of severe or intermediate phenotype.[10] α-L iduronidase deficiency has
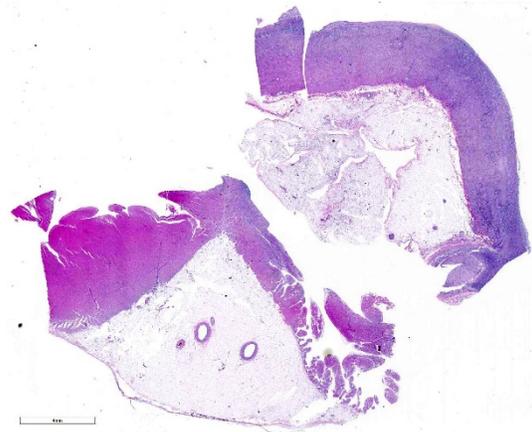
Atrium (left) and aorta (right). Two tissue sections are presented for examination. The wall of the aorta is markedly thickened with abnormal alternating of increased density and pallor at subgross examination. (HE 6X)

been described in dogs,[3, 11, 12] knockout mice,[2] and cats.[4] Even after replacement therapy, there is over a two-fold increase in expression of lysosomal and proteasome function in 19-month-old Plott hounds affected by MPSI.[2] Downregulated were genes associated with cell adhesion, cytoskeleton and calcium regulation. Immunoregulatory genes were also elevated. This could mean that GAGs produce an inflammatory environment that exacerbates disease.[2] Up-regulation of extracellular cathepsin B may also increase pathology due to elastin catabolism.[6]
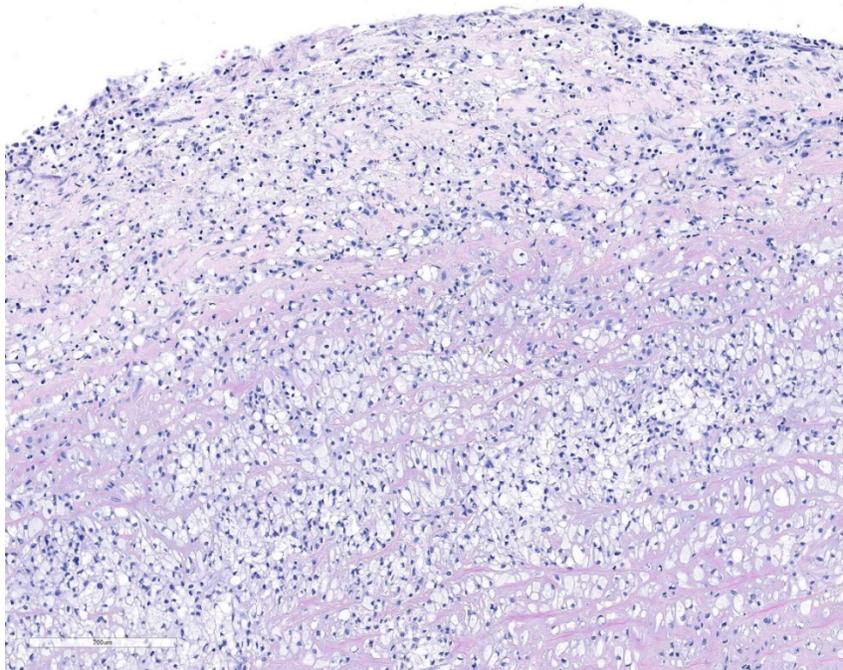
The known mutation in Plott hounds is G to A point mutation in the donor splice site of intron,[4, 8] resulting in retained transcription of intron, but premature termination at the intron-exon junction due to the presence of a stop codon. Homozygous recessives completely lack the enzyme protein or its activity.[8] Mucopolysaccharidosis I has described in a Rottweiler, Afghan hound, this Bassett and a Boston terrier, but information about the specific genetic mutations in these breeds is not known.

Enzyme replacement abrogates part of the clinical syndrome and increases the survival time in humans and dogs, but patients still have a considerable residual disease burden.[1, 10] Enzyme replacement does not correct heart valvulopathy, cardiac stiffness or vasculopathy, and death from cardiac manifestations of disease is common, even after treatment. Bone abnormalities remain, and may require surgical intervention. Dogs given genetically-corrected hematopoietic stem cells had increased GAG clearance, reduced GAGs in the brain and improved

craniofacial appearance. It is noted that people with severe gene mutations like W70X, Q70X and missense A327P, G51D have no functional enzyme activity and the authors indicated that they must be referred for therapy shortly after birth to slow the progression of disease.[10]

Histologically, affected dogs have unstained vacuoles are present in many organs, particularly mesodermal tissues such as fascia, cartilage, blood vessels, heart valves and cerebral leptomeninges.[11]

Lyons examined the branches of the terminal aorta of MPSI-affected dogs that lacked α-L-iduronase enzyme activity.[7] Vascular wall thickness is particularly increased near branch points, locations associated with turbulent flow. Reduced shear stress alters the metabolism of endothelial cells, resulting in increased permeability and leakage. Macrophages may also contribute to degradation of internal elastic lamina, as demonstrated in this case.[7] These asymmetric plaques are characterized by extensive intimal thickening and disruption of the internal elastic lamina, often with significant (60-70%) narrowing of the vascular lumens. Lumenal narrowing was probably more significant in the cases in this study compared to the submitted tissue, because only the terminal branches of the aorta were used in the study. The plaques contained GAG-laden macrophages, fibroblasts and smooth muscle cells, with loss of the endothelial basement membrane and reduced claudin production.[7] CD18+ macrophages were scattered or clustered below the endothelium (Figs. 6, 7). Enzyme treatment makes intimal plaques more

Atrium (left) and aorta (right). Two tissue sections are presented for examination. The wall of the aorta is markedly thickened with abnormal alternating of increased density and pallor at subgross examination. (HE 6X)

JPC Diagnosis: Aorta: Smooth muscle vacuolation, diffuse, severe, with multifocal necrosis **,** intimal histiocytic plaque formation , medial neovascularization, and fibrosis.

JPC Comment: The contributor has done an excellent job in describing the Mucopolysaccharidoses in the dog, and also in man.

The mucopolysaccharidoses are a group of lysosomal storage diseases arising from genetic deficiencies of enzymes needed to catabolize the mucopolysaccharides, a group of glycosamino-glycans constructed by attaching long-chain carbohydrates to proteins. Most of these diseases were first described in humans in the 1970's, and a number of animal models of spontaneous disease have been subsequently identified (Table 1). They are most commonly found in the interstitial ground substance and include dermatan sulfate, chondroitin sufate, keratan sulfate and heparan sulfate. These undegraded or partially degraded glycosaminoglycans accumulate in lysosomes in a number of cells, including macrophages and long-lived post-mitotic cells such as fibroblasts and myocytes.

organized, with reduced macrophages and more laminar organization of fibrous tissue in treated dogs after several months. Similar pathology has been found in human patients and null mice.[1] In affected humans, the disease most commonly affects the coronary arteries. In mice, dilation of the aortic root was more common and coronary artery disease was uncommon; species differences exist in disease manifestations. This progressive vascular changes in MPS-I shares some morphological similarities to atherosclerotic plaques.

Contributing Institution:

Veterinary Medical Diagnostic Laboratory, University of Missouri, 610 East Campus Loop, Columbia MO 65211, http://vmdl.missouri.edu/; http://vpbio.missouri.edu/)
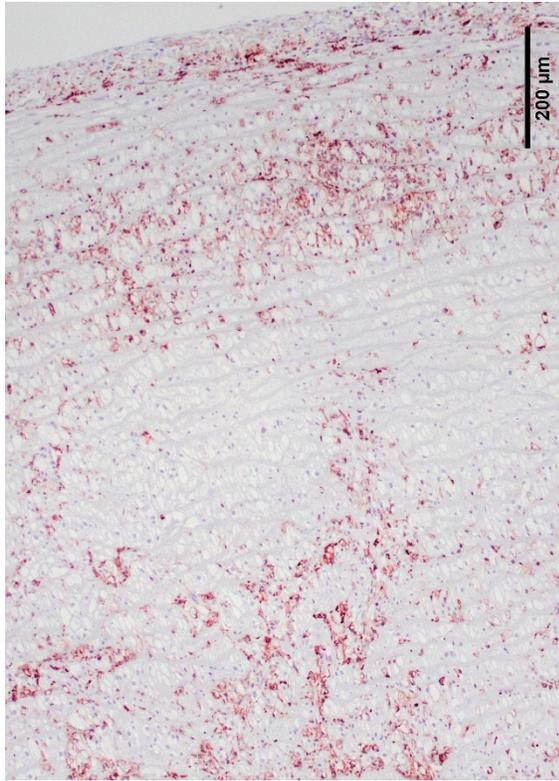
While the accumulation of partially degraded mucopolysaccharides within lysosomes appears histologically to be a relatively benign process largely resulting in

Aorta, dog. Low magnification of a plaque and underlying tunica intima shows the infiltration of the wall by numerous IBA-1- positive histiocytes. (anti IBA-1, 40X). (Photo courtesy of: Veterinary Medical Diagnostic Laboratory, University of Missouri, 610 East Campus Loop, Columbia MO 65211, http://vmdl.missouri.edu/; http://vpbio.missouri.edu/)

cytomegaly, the buildup of these products within lysosomes results in tremendous enlargement and overpopulation of these organelles. This results in hindrance of normal cellular processes, leading to cell death. In addition, the accumulation of autophagic substrate within lysosomes may proceed to a level in which apoptosis may be triggered.

MPS 1, or Hurler's disease, is considered a prototypical, and one of the the most severe forms of mucopolysaccharidoses. It results from a deficiency of α-L-iduronidase, required to hydrolyze the terminal α-L-iduronic acid residues from dermatan and heparan sulfate. In humans, three distinct

clinical manifestations of the condition exist: MPS I H or Hurler's syndrome, MPS I S or Scheie syndrome, and the intermediate phenotypes, collectively referred to as MPS I H/S or Hurler-Scheie syndrome.[9] MPS I H is the most severe, with an early onset (most cases are diagnosed between 6 and 24 months of age) and marked cognitive delay as one of the symptoms. It is a progressive disease which untreated results in death before the 10th year, and includes enlarged liver and spleen, skeletal deformites, coarse faces, and joint stiffness. Affected individuals develop significant hearing loss and an enlarged tongue, along with congnitive delay that relegates affected individuals to only rudimentary language skills. Communicating hydrocephalus often develops at 2-3 years of age. MPS I S, or Scheie syndrome, on the other end of the severity spectrum, is a much more limited phenotype, sharing joint stiffness (an early and often presenting sign), aortic valve disease, corneal clouding and other ocular abnormalities, but not the cognitive delay, and diagnosis is often made between 10-20 years of age.[9]

Treatment of Hurler's disease has advanced dramatically in recent years, and includes allogeneic hematopoietic stem cell transplants (HSCT) and enyme replacement therapy with human recombinant laronidase.[10] HSCT is considered the most appropriate treatment for MPS I H, and has been shown to be successful in halting progression of cognitive delay when used in patients before 2.5 years of age. Enzyme replacement therapy has been shown to be effective in cases of MPS I S and may be initiated in more severely affected individuals prior to more definitive HSCT; however, it is not recommended for Hurler's syndrome due to the limited ability of laronidase to cross the blood-brain barrier.[10]
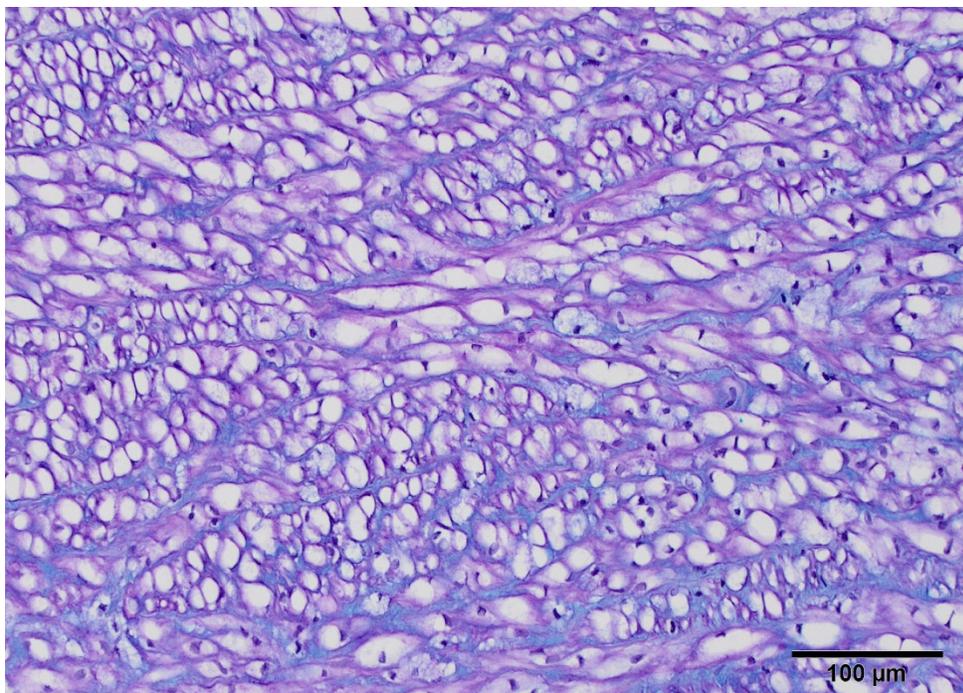
An Alcian blue 2.5 stain demonstrates accumulation of mucinous extracellular matrix in the wall of the aorta (MEMA – mucinous extracellular matrix accumulation.) (Alcian blue 2.5, 400X)

References:

1. Braunlin E, Mackey-Bojack S, Oanoskaltsis A, et al. Cardiac functional and histopathologic findings in humans and mice with mucopolysaccharidosis type I: implications for assessment of therapeutic interventions in Hurler syndrome. Pediatr Res. 2006;59:27-32.

2. Gonzalez EA, Martins GR, Tavares AMV, et al. Cathepsin B inhibition attenuates cardiovascular pathology in mucopolysaccharidosis I mice.Lice Science. 2018;196:102-109.

3. Haskins ME. Animal models of mucopolysaccharidosis and their clinical relevance. *Acta Paediatr*. 2007;96:56-92.

4. Haskins ME, Aguirre GD, Jezyk PF, Desnick RJ, Patterson DF. The pathology of the feline model of mucopolysaccharidosis I. *Am J Pathol.* 1983:112:27-36.

5. Hinderer C, Katz N, Louboutin J-P, et al. Abnormal polyamine metabolism is unique to the neuropathic forms of MPS: potential for biomarker development and insight into pathogenesis. *Human Molec Genet.* 2017; 26:3837-3849.

6. Khalid O, Vera MU, Gordts PL, et al. Immune-mediated inflammation may contribute to the pathogenesis of cardiovascular disease in mucopolysaccharidosis. *Plos One.* 2016;DOI:10.1371/journal.pone.010850.

7. Lyons JA, Dickson PI, Wall JS, et al. Arterial pathology in canine mucopolysaccharidosis-I and response to therapy. Lab Invest. 2010;91:665-674.

8. Menon KP, Tieu PT, Neufeld EF. Architecture of the canine IDUA gene and mutation underlying canine mucopolysaccharidosis I. Genomics 1992;14:763-768.

dosis I. Genomics 1992; 14:763-768.

9. Neufeld E, Muenzer JA. The mucopolysaccharidoses. Ch 61 in

Eds. Scriver CR, Beaudet AL, Sly WS,Valle D. *The Metabolic Basis of Inherited Disease, vol 2*, 6th ed. UDA:McGraw-Hill; 1989:1565-1587.

10. Parini R, Deodoro F, Di Rocco M, et al. Open issues in mucopolysaccharidosis I-Hurler. *Orphanet J Rare Dis*. 2017;12:112. DOI 10.1186/s13023-017-0662-9.

11. Shull RM, Helman RG, Spellacy E, Constantopoulos G. Munger RJ, Neufeld EF. Morphologic and biochemical studies of canine mucopolysaccharidosis I. *Am J Pathol*. 1984;114:487-495.

12. Spellacy E, Shull RM, Constantopoulos G, Neufeld EF. A canine model of human alpha-L-iduronidase deficiency. *Proc Natl Acad Sci USA*. 1983;80:6091-3065.